Pickering Emulsion Approach: A Novel Strategy to Fabricate Waterborne Polyurethane with Enhanced Abradability and Water-resistance Comparable to that of Solvent-based Coating

Xiaobo Wu[a, b], Jianhui Wua, b, Changdao Mu[c], Chunhua Wang[a, b]*, Wei Lin[a, b]

a. Department of Biomass and Leather Engineering, Key Laboratory of Leather Chemistry and Engineering of Ministry of Education, Sichuan University, Chengdu 610065, China,

b. National Engineering Laboratory for Clean Technology of Leather Manufacture, Sichuan University, Chengdu 610065, China,

c. Department of Pharmaceutics and Bioengineering, School of Chemical Engineering, Sichuan University, Chengdu 610065, China

Abstract

The urgent requirement of replacement for solvent polyurethane (PU) makes waterborne polyurethane (WPU) coating more attractive and popular in many industrial areas. However, the simultaneous realization of good dispersion stability and high performance of the cured films especially water resistance remains challenging. Herein, we propose a novel and facile Pickering emulsion approach to fabricate WPU with enhanced abradability and water-resistance comparable to that of solvent-based PU coating. In this approach, the hydrophobic polyurethane synthesized by poly-addition reaction in ethyl acetate is directly dispersed into water with SiO_2 nanoparticles as Pickering stabilizer followed by subsequent evaporation of the remaining solvent to obtain Pickering waterborne polyurethane dispersion (PWPU dispersion). The ability of SiO_2 to stabilize emulsion can be modulated by hydrophobic modification with propyltriethoxysilane (PTS). SiO_2 nanoparticles with an optimal PTS-grafting rate of 2.8 wt% enables the PWPU dispersion with excellent long-term, chemical, thermal, and freeze-thaw stability. The highly-transparent composite films with honeycomb structures are readily formed by casting PWPU dispersion at room temperature. The thermal and mechanical properties of PWPU films are comparable to or superior to solvent-borne polyurethane (SPU) and self-emulsifying waterborne polyurethane (SWPU) films. Moreover, the water absorption of the PWPU-5 film is approximately 20 times lower than that of SWPU, demonstrating the excellent water-resistance. We further validated the coating performance of PWPU for leather finishing. The hydrophobicity, abrasion resistance and water vapor permeability of PWPU-coated leather are superior to those of SPU and SWPU-coated leather.

Keywords: Pickering emulsion approach; Waterborne polyurethane; Emulsion stability; Abradability; Water-resistance; Leather coating

1. Introduction

Polyurethanes (PU) are widely used as an importance coating material in many industries including textile and leather garment[1], biomedical implants[2], automotive and marine applications[3] due to their advantages of strong designability, excellent film-forming ability and wide range of physical-chemical properties. In the past decades, solvent-based polyurethane has been mainly replaced with waterborne polyurethane (WPU) as a consequence of the enforcement of more stringent environmental and occupational health and safety regulations.[4-6] Therefore, WPU have drawn great significance and been extensively researched for a long time.[7-9] To disperse hydrophobic polyurethane into water, emulsification is the key process, affecting the emulsion stability and overall properties of the cured films. Up to now, WPU emulsions are prepared by either self-emulsification method in the presence of incorporated hydrophilic groups or by mechanical emulsification with the help of small molecular surfactants.[10] While the two emulsification methods would lead to poorer film performance of WPU especially the water resistant-property compared with those of solvent-based PU because of the presence of hydrophilic components.[11] Moreover, surfactants are deleterious for film applications due to the inevitable migration to the interfaces of the cured films, resulting in the reduced optical transparency, gloss and adhesion[12] and even the low mechanical strength[13], which are very important properties for their real applications such as leather finishing.

Particle-stabilized emulsions, also known as Pickering emulsions, have gained widespread attention recently as they have a significant advantage over traditional surfactant-stabilized emulsion especially in the outstanding stability against coalescence brought about by the high desorption energies of solid particles[14]. As a result, Pickering emulsion approach have been reported to fabricate versatile colloidosomes including emulsions[15], microcapsules[16], and Janus particles[17]. Current researches further reported the waterborne polymer dispersions stabilized by Pickering stabilizer, such as waterborne polydimethylsiloxane and epoxy resin Pickering emulsions.[18-20] As for these Pickering emulsions for forming a film, publications have demonstrated the double functions of Pickering stabilizer, i.e., emulsification and mechanical reinforcement [6], which is desirable for waterborne coatings including WPU. The Pickering emulsion approach can be employed to eliminate the limits brought about by traditional surfactants or the introduction of hydrophilic groups in the fabricating process of traditional WPU, while combing the advantages of Pickering stabilizer. However, using Pickering emulsion approach to achieve the dispersion of polyurethane in water is rarely reported and little study is conducted on WPU films formed directly from Pickering emulsions systems. If a polymer Pickering emulsion is used to form a film, the interaction between the Pickering

stabilizer and the polymer matrix as well as the film-formation process must be explored.

In the present study, we have achieved the dispersion of hydrophobic polyurethane in water via Pickering emulsion approach and fabricated the SiO_2-stabilized WPU dispersion (named as PWPU dispersion). The hydrophobic polyurethane has been synthesized via a polyaddition polymerization reaction using ethyl acetate as solvent. SiO_2 nanoparticles were chosen as the Pickering stabilizer to emulsify the polyurethane due to their distinct advantages of commercial availability, low cost and easy modification.[19] Since the introduction of inorganic particles (i.e., SiO_2) into WPU via Pickering emulsion approach in this study is very different from the previously-reported methods for the preparation of traditional waterborne polyurethane nanocomposites[21], we focus on the effect of SiO_2 on emulsification process in the systems containing polyurethane solution as oil phase, emulsion stability, structures and properties of the cured PWPU films. The solvent-borne polyurethane (SPU) and self-emulsifying waterborne polyurethane (SWPU) were also synthesized as controls. Furthermore, the PUs was employed in the finishing process of tanned leather and the applied performance of the coated leather including hydrophobicity, abrasion resistance, and water vapor permeability were evaluated.

2. Experimental

2.1. Materials

Fumed SiO_2 nanoparticles (99.5%, 20±5 nm) were obtained from Macklin (Shanghai). Propyltrimethoxysilane (PTS, > 98%) and isophorone diisocyanate (IPDI, 99%) were obtained from Adamas (Shanghai). Polytetrahydrofuran (PTMG, Mn~2000), dimethylol propionic acid (DMPA, 98%), and rhodamine B (98%) were obtained from Aladdin (Shanghai). 1, 4-butanediol (1, 4-BDO, 99%), dibutyltin dilaurate (DBTDL, 95%), Triethylamine (TEA, 99%), absolute ethyl alcohol (≥99.5%), ethyl acetate (99.5%), ethanol absolute (≥99.7%) and lauryl sodium sulfate (SDS, ≥98%) were purchased from Chengdu Kelong. Chemical Reagent Factory. PTMG, and 1, 4-BDO were dried under reduced pressure at 100℃ for 2 h prior to use. Goatskin crust leathers were self-made in our laboratory. All other reagents and solvents were used as received.

2.2. Modification of SiO_2 nanoparticles with PTS

A series of modified SiO_2 nanoparticles (named as SiO_2-x) were prepared in this study. The value of x denotes the mass ratio (wt%) of PTS to SiO_2 nanoparticles. The SiO_2 nanoparticles were modified with PTS in an aqueous ethanol solution. Specifically, the preparation process of SiO_2-2.8 was described as follows. 3 g of SiO_2 nanoparticles was dispersed in 59.25 g ethanol. 0.750 g of deionized water and 1.50 g of PTS were added and mixed with the SiO_2 ethanol dispersion. Afterward, the mixture was vigorously stirred at 65 °C for 8 h. The modified SiO_2 nanoparticles were obtained after the washing with ethanol for three times to remove excess PTS and subsequent drying in a vacuum drying oven at 70°C for 12 hours. The characterization data are summarized in Table S1. FT-IR spectra of modified SiO_2 nanoparticles: 475 cm^{-1}, 810 cm^{-1}, 1000, and 1100 cm^{-1} (Si-O-Si), 980 cm^{-1} and 3430 cm^{-1} (Si-OH), 2870 cm^{-1} (C-H_2), 2960 cm^{-1} (C-H_3).

2.3. Synthesis of solvent-based polyurethane and self-emulsifying waterborne polyurethane

Solvent-based polyurethane (SPU) and self-emulsifying waterborne polyurethane (SWPU) were synthesized via a polyaddition polymerization reaction in ethyl acetate under a nitrogen atmosphere. In detail, for SPU, IPDI was reacted with anhydrous PTMG at 80°C for 1 h to obtain an isocyanate-terminated prepolymer. Then, 1,4-BDO were added as chain extenders, and DBTDL was added dropwise as a catalyst. The reaction was conducted at 70 °C for 2 h and SPU solution with a concentration of approximately 20% was obtained. In the case of SWPU, DMPA was added to react with prepolymer for 1 h before adding 1,4-BDO. After the completion of reaction with 1,4-BDO, TEA was added to neutralize the carboxyl groups in WPU for 30 min at 50 °C. Then, the mixture was dispersed in deionized water by a homogenizer for 10 min under high-speed shearing. SWPU dispersion with a solid content of approximately 20% was obtained after the removal of residual ethyl acetate by rotating distillation. The formulations of SPU and SWPU are summarized in Table S2. FT-IR spectra of SPU: 1105 cm^{-1} (C-O-C), 1710 cm^{-1} (C=O), 2870 cm^{-1} (C-H_2), 2960 cm^{-1} (C-H_3), 3323 cm^{-1} (N-H). ^{1}H NMR spectra of SPU (400 MHz, deuterated DMSO, ppm): 0.93 (m), 1.06 (p), 1.08 (l), 1.24 (h), 1.50 (f), 1.57 (n), 2.18 (b), 2.72 (j), 3.11 (k), 3.33 (e), 3.57 (i), 3.94 (g), 4.36 (a), and 7.00 (cd). FT-IR spectra of SWPU: 1105 cm^{-1} (C-O-C), 1710 cm^{-1} (C=O), 2870 cm^{-1} (C-H_2), 2960 cm^{-1} (C-H_3), 3323 cm^{-1} (N-H). ^{1}H NMR spectra of SWPU (400 MHz, deuterated DMSO, ppm): 0.93 (m), 1.06 (p), 1.07 (p) 1.08 (l), 1.24 (h), 1.50 (f), 1.57 (n), 2.18 (b), 2.72 (j), 3.11 (k), 3.33 (e), 3.57 (i), 3.94 (g), 4.36 (ao), and 7.00 (cd). FT-IR spectra of PWPU: 1000 cm^{-1} (Si-O-Si), 1100 cm^{-1} (Si-O-Si), 1105 cm^{-1} (C-O-C), 1710 cm^{-1} (C=O), 2870 cm^{-1} (C-H_2), 2960 cm^{-1} (C-H_3), 3323 cm^{-1} (N-H).

2.4. Preparation of waterborne polyurethane via Pickering emulsion approach

Schematic illustration of the Pickering emulsion approach to prepare WPU dispersion was shown in Figure 1. SiO_2-x nanoparticles with the appropriate solid content were prepared by diluting with Milli-Q water. A series of PWPU dispersions were obtained by the following steps. First, the SiO_2-x nanoparticles with the appropriate content was mixed with a certain amount of SPU solution (ethyl acetate as solvent) and then the mixture was emulsified with a homogeneous emulsifier at 15000 rpm for 10 s and at 13500 rpm for 10 s. Afterwards, the crude PWPU dispersions were obtained by evaporating the ethyl acetate of the resulting emulsions at a vacuum of 0.08 MPa and a temperature of

50°C. Finally, the crude PWPU dispersions were filtered through a 100-mesh sieve to obtain PWPU dispersions. The conversion rate of the PWPU dispersions was calculated using Eq. (1):

$$\text{Conversion rate } (\%) = (m_2)/m_1 \times 100\% \quad (1)$$

where m_1 and m_2 are the weight of PWPU dispersion before and after filtration, respectively.

The solid content of the PWPU dispersions was calculated using Eq. (2):

$$\text{Solid content } (\%) = (m_2)/m_1 \times 100\% \quad (2)$$

where m_1 and m_2 are the weight of PWPU dispersion before and after drying, respectively.

Another Pickering emulsion stabilized by 1 wt% rhodamine B-labeled SiO_2-2.8 was prepared for confocal laser scanning microscopy (CLSM) observation. The rhodamine B was dissolved in absolute alcohol at a concentration of 1 mg/mL. Subsequently, the dye solution was added to the dispersion of SiO_2-2.8 nanoparticles, and the mixture was stirred at room temperature for 24 h. The rhodamine B-labeled SiO_2-2.8 nanoparticles were then collected and purified by centrifugation, followed by washing with absolute alcohol for three times. Finally, those labeled SiO_2-2.8 were utilized as stabilizers for Pickering emulsion, with a PU dissolved in ethyl acetate as the oil phase.

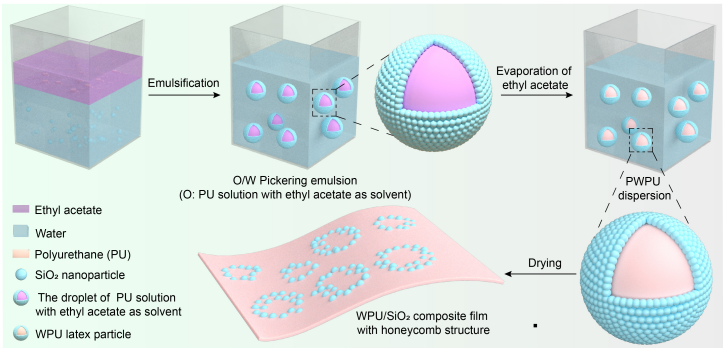

Figure 1. Schematic illustration of the Pickering emulsion approach to prepare WPU dispersion and form composite film.

2.5. Preparation of films

The films were prepared by pouring a designated mass of SPU solution, SWPU and PWPU dispersions into cleaned polytetrafluoroethylene (PTFE) moulds followed by drying at room temperature until reaching a constant weight (Figure 1). The obtained PWPU composite films were denoted as PWPU-x, where x represents the weight percent of SiO_2-2.8 nanoparticles in the dried film.

2.6 Application in leather coating

8 g of PWPU dispersion stabilized by 1.0 wt% SiO_2-2.8 (solid content is 20%) was sprayed on goatskin crust leathers with a diameter of 6 cm, following by drying at 30 ℃ for 48 h to obtain PWPU-5 coated leather. Meanwhile, the leather coated by SPU, and SWPU under the same condition were used as control samples.

2.7 Characterization

FT-IR spectra were observed using a Thermo Fisher Scientific Nicolet iS10 IR spectrometer. The SiO_2 nanoparticles were measured by potassium bromide method, while the SPU, SWPU, and PWPU composite films were measured directly. For each sample, 64 scans were performed at a resolution of 4 cm^{-1} ranging from 400 cm^{-1} to 4000 cm^{-1}. ^1H NMR spectra of SPU and SWPU were observed using a Bruker AV II 400 MHz NMR spectrometer at room temperature with deuterated dimethyl sulfoxide (DMSO) as the solvent and tetramethyl silane (TMS) as the internal standard. Thermogravimetric analysis (TGA) of SiO_2 nanoparticles, and the films was performed on a TG209F1 instrument under nitrogen atmosphere from 100°C to 800°C at a heating rate of 10 °C/min. The grafting rate of PTS on SiO_2 nanoparticles was calculated using Eq. (2):

$$\text{Grafting rate (wt\%)} = (m_1 - m_3)/(m_2 + m_3) \times 100\% \quad (2)$$

where m_1 stands for the percentage mass loss of the modified SiO_2 nanoparticles at 800 °C in wt%, m_2 stands for the percentage residual mass of the modified SiO_2 nanoparticles at 800 °C in wt%, and m_3 stands for the mass loss of unmodified SiO_2 nanoparticles in wt%.

Drop test was used to infer the emulsion type. The Pickering emulsions were added dropwise to deionized water. An oil-in-water (O/W) emulsion readily disperses in water and *vice versa*. The WCAs of SiO_2-x nanoparticles and the coated leather surfaces were determined by using the sessile drop method at room temperature with a telescoping goniometer (OCA15EC, DataPhysics) equipped with video capture. For SiO_2-x nanoparticles, 0.1 wt% SiO_2-x nanoparticle dispersions were dripped on the silicon wafer and thoroughly dried at room temperature to form a multilayer structure of nanoparticles on the substrate. Then, a 3 μL of distilled water drop was dripped on the wafer surface in ethyl acetate medium. For the coated leather, a 5 μL of distilled water was pumped from a microsyringe onto their

surfaces. All the images were captured using the telescope fitted with the video camera. Each WCA value was expressed as the average value of three independent measurements at different locations of the same sample.

Microscope images of the PWPU dispersions were obtained using an optical microscope (CX41, Olympus) with a 40 × objective. All samples were dropped onto cover slides and the x/y layers were scanned. All images were taken one day after preparation. The Pickering emulsion stabilized by 1 wt% rhodamine B-labeled SiO_2-2.8 nanoparticles was imaged using a CLSM (Stellaris 5, Leica) equipped with a 20× air objective and 40× oil immersion objective. The labeled SiO_2-2.8 nanoparticles were excited by lasers emitting at 561 nm. Prior to observation, the PWPU dispersions were deposited onto a cover glass, followed by scanning using the laser.

The long-term storage stability of PWPU dispersions containing 1.0 wt% SiO_2-2.8 were evaluated by storing them at room temperature for 60 d. The chemical and thermal stability of PWPU dispersions were then evaluated according to the industrial standard QB/T 2223-1996.[22] Finally, the freeze-thaw stability of PWPU dispersions was tested according to GB/T 11175-2021.[23] The size and distribution of PWPU dispersions were measured by using a laser particle sizer (Mastersize 2000, Malvern Instruments Inc.). PWPU dispersions were diluted to 10^{-3} wt% with Milli-Q water before test. Each sample was repeated three times.The number-average molecular weight (Mn) and corresponding polydispersity index (PDI) of the PWPU-5.0 film were determined using GPC (Rid-20A, Shimadzu) at a temperature of 35 °C on a TSKgel GMPWXL column, employing a series of monodisperse polystyrenes as standard samples and tetrahydrofuran (THF) as the mobile phase with a flow rate of 1.0 mL/min. Thin samples (thinckness = 0.1 cm) were obtained by cutting parallel or perpendicular to the plane of SWPU, SPU and PWPU films using an EM FC6 ultramicrotome (Leica, Switzerland) cooled with liquid nitrogen at −90 °C. Then, the cross-section or surface morphologies of the samples were imaged using field emission scanning electron microscopy (Inspect F50, FEI) with an accelerating voltage of 15 KV. Each sample was sputtered with gold before test.

The stress-strain curves, tensile strength (TS) and elongation at break (EB) of polyurethane samples were evaluated with an electronic universal testing machine (CMT6202, Meters Industrial Systems (China) Co., Ltd.) according to the standard testing method ASTM D882-97.[24] Two rectangular strips (width 1.8 mm, length 34 mm) were cut from each film to determine the mechanical property. Initial grip separation was set at 34 mm and stretching rate was at 100 mm/min. TS (MPa) was calculated from $TS=F_{max}/A$, in which F_{max} stands for the maximum load (N) needed to pull the sample apart, and A stands for cross-sectional area (m^2) of the samples. EB (100%) was calculated by EB=L/13.3, in which L stands for the elongation of each film at rupture (mm), and 13.3 stand for the initial grip length (mm) of each sample. The testing was conducted twice for each sample.

The gravimetric method was used to test the water absorption rate of polyurethane films. Pieces of films (1 cm×1 cm) were accurately weighed (wet weight without excess of water), immersed in distilled water at room temperature for 24 h. The WAR of film was calculated using the following Eq. (3):

$$WAR\ (\text{wt\%}) = (m_2 - m_1)/m_1 \times 100\% \quad (3)$$

where m_2 and m_1 were the wight of the film after and before water absorption, respectively.

The abrasion resistance of coated leathers was evaluated with an abraser (YL-3315T1, PW Instruments (Guangdong) Co., Ltd) according to the standard testing method QB/T 2726-2005. Each sample with diameter of 106 ± 1 mm was rubbed for 2500 cycles at a rotation speed of 60 rpm under a load of 500 g, then the final weight was recorded. Wear mass loss was calculated using Eq. (4):

$$\text{Wear mass loss (mg)} = m_1 - m_2 \quad (4)$$

where m_1 and m_2 were the mass of the sample before and after abrasion test, respectively. Each wear mass loss value was expressed as the average value of three independent measurements.

The WVP of the coated leathers was measured according to the standard testing method GB/T 1037–2021. The samples with a thickness of 2.5 mm and a diameter of 60 mm were sealed to the open mouth of a test dish containing calcium chloride and then placed in a constant relative humidity (90%) desiccator at 38℃ for 24 h. Calcium chloride was dried under reduced pressure at 200℃ for 2 h prior to use. The WVP of the samples were calculated using Eq. (5):

$$\text{WVP}\ (\text{g}/\text{m}^2 \cdot 24\text{h}) = \Delta\text{m}/\text{A} \quad (5)$$

where Δm was the mass variation of calcium chloride after 24 h, A was the exposure area of the samples with a diameter of 40 mm. Each WVP value was expressed as the average value of three independent measurements.

3. Results and discussion

3.1. Characterization of SiO_2-x nanoparticles and the synthesized polyurethane

PTS were used to modify SiO_2 nanoparticles to improve its emulsifying ability. In contrast to unmodified SiO_2, new weak absorption peaks at 2870 cm^{-1} and 2960 cm^{-1} appeared in the FT-IR spectra of SiO_2-x, corresponding to the antisymmetric stretching vibration of C-H_2 and C-H_3, respectively (Figure 2a).[25] The result indicate the successful grafting of PTS onto the surface of SiO_2 nanoparticles. In order to quantify the grafting rate of PTS, the SiO_2 nanoparticles were analyzed

by TGA. A total mass loss of unmodified SiO_2 at 800°C is 0.4 wt%, which is caused by the condensed dehydration of the Si-OH[26]. For SiO_2-x, the mass loss increases with the increasing amount of PTS at the same temperature (Figure 2b). The grafting rates of PTS on SiO_2 nanoparticles are 1.5 wt%, 2.8 wt%, and 4.2 wt%, respectively (Table S1). In the FT-IR spectra of SPU and SWPU, absorption peaks at 1710 cm^{-1} and 3323 cm^{-1} are assigned to the C=O and N-H stretching vibration of urethane bond, respectively, which are the characteristic peaks of polyurethane (Figure 2c).[27] Besides, the signal of the protons in urethane bond (δ = 7.00 ppm (cd)) appear in the ^{1}H NMR spectra of SPU and SWPU (Figure 2d).[28] Unlike SPU, new peaks at δ = 1.06 ppm (p) and δ = 4.08 ppm (o) attribute to the protons in CH_3 and CH_2 of hydrophilic chain extender DMPA are observed in the ^{1}H NMR spectra of SWPU.[29] All these facts above manifest the successful synthesis of SPU and SWPU.

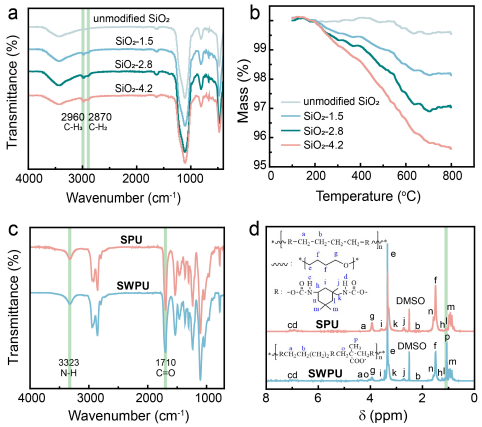

Figure 2 (**a**) FT-IR and **(b)** TGA curves of SiO_2-x nanoparticles. **(c)** FT-IR and **(d)** ^{1}H NMR spectra of SPU and SWPU.

3.2 Effect of SiO_2-x and its concentration on the emulsion and PWPU dispersion

SiO_2 nanoparticles with different PTS-grafting rate were used to stabilize the emulsion with the PU dissolved in ethyl acetate as the oil phase. The unmodified SiO_2 fails to stabilize the emulsion as the corresponding emulsions quickly delaminate. However, stable emulsions were obtained when using modified SiO_2 as Pickering stabilizer, indicating their good ability to stabilize the emulsion. This can be attributed to the fact that hydrophilic feature of unmodified SiO_2 (WCA = 28 ± 3°) makes it difficult to adsorb onto oil-water interface (Figure 3a). In contrast, the modified SiO_2 has proper wettability facilitating their adsorption at the oil-water interface to obtain stable Pickering emulsions (Figures 3b-d). Dilution experiments were used to verify the type of the resulting emulsions. The emulsion stabilized by SiO_2-2.8 can remain dispersed in water, while the emulsion stabilized by SiO_2-4.2 fails, indicating the former is of the oil-in-water type and the latter is of water-in-oil type. The reason is that the WCAs of SiO_2-1.5 and SiO_2-2.8 are 75° ± 1° and 84° ± 2°, respectively, which confer better affinity to the aqueous phase, resulting in the formation of the oil-in-water emulsion (Figure 3b-c). SiO_2-4.2 exhibits a higher WCA (111° ± 1°) due to the presence of higher amount of hydrophobic PTS on SiO_2, rendering it more prone to be immersed in the oil phase and facilitating the formation of a water-in-oil emulsion (Figure 3d).[25, 30] Therefore, SiO_2-2.8 was selected as Pickering emulsifiers for the subsequent experiments in consideration of WPU dispersion type and the benefit of water resistance of polyurethane film.

During the preparation of the emulsions with different content of SiO_2-2.8, it is found that the polyurethane fails to be dispersed in water in the absence of SiO_2-2.8, with both oil and water phase separation occurring immediately after emulsification. In contrast, stable emulsions can be formed when the dosage of SiO_2-2.8 exceeds 0.5 wt%). After evaporating the ethyl acetate of the emulsions, the PWPU dispersions were obtained. Optical microscope shows that folds on the surface of the WPU latex particles (Figure 3e-h), which is possibly related to the absorption of SiO_2 at the PU-water interface. The microstructures of the Pickering emulsions stabilized by rhodamine B-labeled SiO_2-2.8 nanoparticles are intuitively observed using CLSM because the labeled nanoparticles can be excited at 561 nm in red. The typical CLSM images clearly exhibit that almost all nanoparticles anchor on the PU/water interface and little nanoparticles is in the continuous phase (Figures i-j).[31] The removal of ethyl acetate leads to a slight decrease in the size of the dispersion phase from 28±1 μm to 24±1 μm (Table S3), consequently resulting in the formation of wrinkles (Figures 3e-h). However, the PWPU dispersion still maintains good stability. This can be attributed to that the hydroxyl groups on the surface of SiO_2-2.8 is capable of forming hydrogen bond interactions with both the urethane bond on the hard segment and the ether bond on the soft segment of polyurethane[21] (Figure 3k), preventing the desorption of SiO_2-2.8 from the interface between PU and water during the desolventizing process[32].

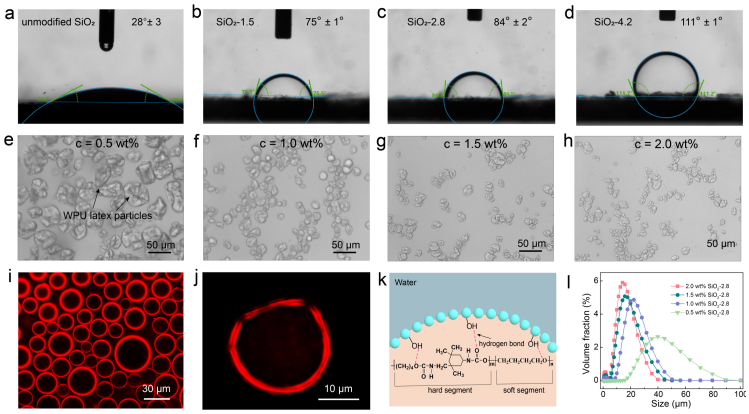

Figure 3 (**a-d**) WCA of unmodified SiO_2 nanoparticles and SiO_2-x nanoparticles in the ethyl acetate. **(e-h)** Optical micrographs of PWPU dispersions stabilized by different SiO_2-2.8 concentration. **(i-j)** CLSM images of Pickering emulsion with a PU dissolved in ethyl acetate as the oil phase, stabilized by 1 wt% rhodamine B-labeled SiO_2-2.8 nanoparticles. **(k)** Schematic illustration of the hydrogen bond interactions between SiO_2-2.8 and polyurethane. **(l)** size distributions of the WPU latex particles in PWPU dispersions stabilized by different SiO_2-2.8 concentration.

With the dosage of SiO_2-2.8 increasing from 0.5 wt% to 2.0 wt%, the solid content and mean size of the WPU latex particles of PWPU dispersions exhibit an increment from 17.0 ± 0.5% to 24.1 ± 0.3% and a reduction from 45±1 μm to 17±1 μm, respectively. (Figure 3l and Table S3). This can be attributed to the fact that the increased SiO_2-2.8 nanoparticles enables the stabilization of a greater amount of oil phase and larger oil/water interfaces at a constant oil-water ratio, thereby facilitating the achievement of higher solid content and smaller particle size WPU latex particles[28]. The conversion rate of the PWPU dispersions is above 94% when the content of SiO_2-2.8 exceeds 1.0 wt% (Table S3), indicating that PWPU dispersion with high conversion rate can be obtained via Pickering emulsion approach. Although the mean size of the WPU latex particles in PWPU dispersions is larger than that of SWPU, all the PWPU composite films possess high transparency, which is almost comparable to that of the SWPU and SPU films. This is due to the small size and high degree of dispersion of SiO_2-2.8 nanoparticles within the films achieved via the Pickering emulsion approach.

3.3 Stability of PWPU dispersion

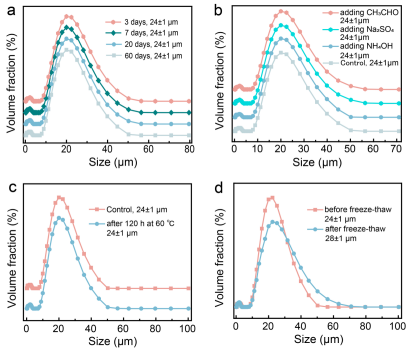

Figure 4 Mean size and distribution of the WPU latex particles in PWPU dispersion stabilized by 1.0 wt% SiO_2-2.8 after **(a)** storage for 3-60 days, (**b**) adding different chemicals, **(c)** heating for 120 h at 60 °C, and **(d)** three tests of freeze-thaw.

As expect, the mean size of the WPU latex particles is 24 ± 1 μm after storing the PWU emulsion at room temperature for 60 days, which is almost unchanged compared with freshly prepared one (Figure 4a), indicating its excellent long-term stability. As shown in Figure 4b-c, the mean size of the WPU latex particles in PWPU dispersion remains unchanged after adding different chemicals (CH_3CHO, Na_2SO_4, NH_4OH), or storing at 60°C for 120 h, suggesting the chemical stability and thermal stability of PWPU dispersion meet the requirement of QB/T 2223-1996. The freeze-thaw stability of PWPU dispersion was illustrated in Figure 4d. The unchanged mean size of the WPU latex particles after three tests of freeze-thaw implies the good freeze-thaw stability. The good stability of PWPU dispersion is as expected because the adsorption SiO_2-2.8 nanoparticles adsorb at the interface of polyurethane and water is irreversible[33, 34] and the particles can form a dense particle film at the oil-water interface, acting as a physical barrier effectively to prevent the WPU latex particles from agglomerating or contacting with chemicals[35]. Overall, the stability of PWPU dispersion meet the requirement of industrial/national standards on leather finishing agents.

3.4 Structures, morphologies and formation mechanism of PWPU composite films

The effects of SiO_2-2.8 nanoparticles on the structure of PWPU composite films was investigated by FT-IR. Compared with SWPU, the appearance of a new peak at 1000 cm−1 in PWPU, which can be attributed to the antisymmetric stretching vibration of Si–O–Si, indicates the presence of SiO_2-2.8 nanoparticles in the composite films(Figures 5a-b).[36] In addition, another peak of the antisymmetric stretching vibration of Si–O–Si at about 1100 cm^{-1} is overlapped by the stretching vibration of O–C–O in SPU.[37] A red-shift in the peak position from 1109 cm^{-1} to 1098 cm−1 (towards lower wavenumbers) is observed as the SiO_2-2.8 content increases from 0.0% to 10.0%, which is possibly related to the interface interactions (i.e., hydrogen bonding) between the two components.[37] The molecular weight and its distribution are crucial factors affecting the physicochemical properties of polyurethane materials. The Mn and PDI of the PWPU-5.0 are 62520 g/mol and 1.84, respectively (Figure 5c), which surpass those of the reported WPU leather coating [38, 39], indicating that PWPU-5.0 is a suitable candidate as leather coating.

In order to investigate formation mechanism of PWPU composite films, cross-sectional morphologies of SPU and PWPU films was observed. The cross-section of SWPU film is flat and clean, and no SiO_2-2.8 nanoparticle boundary is observed (Figure 5d). In contrast, PWPU composite films resembled a striking honeycomb structure with thick wall (Figure 5e-g), which is consistent with the results reported in the previous literatures.[40-44] The fact is that this honeycomb structure is formed by SiO_2-2.8 nanoparticles that absorbed at the oil/water interface. The thickness of the honeycomb walls within the film was calculated using software Nano Measurer 1.2 and the results were shown in Figure 5h-j. Clearly, at higher content of SiO_2-2.8 (PWPU-7.5), larger thickness of the honeycomb wall is observed, indicate that more SiO_2-2.8 absorb at polyurethane/water interface. Moreover, such a heterogenous covering and the formation of good films from PWPU dispersion suggesting that the presence of absorbed SiO_2 at WPU latex particles during film formation process seems not to be an impediment for the interdiffusion of polyurethane chains between the WPU latex particles with the casting temperature of 25 ℃ (i.e., room temperature).

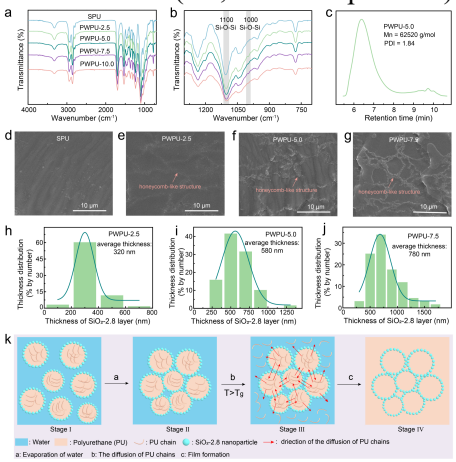

Figure 5 FT-IR spectra of SPU and PWPU films ranging from **(a)** 4000 to 700 cm^{-1} and **(b)** 1300 to 700 cm^{-1}. **(c)** GPC trace of PWPU-5.0. **(d-g)** The SEM images of cross-sectional morphologies of SPU and PWPU films. **(h-j)** Thickness distributions of honeycomb walls in PWPU films. **(k)** Schematic illustration of film formation process of PWPU dispersion.

The film formation process of PWPU dispersion occurs in four main stages as illustrated in Figure 5k. Stage I corresponds to the waterborne polyurethane dispersion stabilized by SiO_2 (i.e., PWPU dispersion). In stage II, the WPU latex particles start come to contact by evaporating water gradually, forming a close packed array with water-filled interstices. Stage III is referred to the formation of a densely packed array in which interstitial water is lost and polyurethane chains begin to interdiffuse progressively across the boundaries of SiO_2-2.8 nanoparticles under the action of capillary forces and van der Waals forces. Stage IV is defined by a composite film with heterogenous structure formed as a consequence of the interdiffusion of polyurethane chain ends and the formation of entanglements across the particle boundaries. The transition from II to III is very important for forming PWPU composite film, which can only occur when the temperature above the glass transition temperature (T_g) of the polyurethane. DSC thermogram shows that T_g values of PWPU films (-75 ℃–-72 ℃) is far below their film-forming temperature (i.e., room temperature). PWPU dispersions exhibit the advantage of being capable to form composite film under low temperature, which is beneficial to their real film applications.

3.5 Thermal and mechanical properties, water resistance of PWPU composite films

Thermal stability is valuable parameters in the practical applications of WPU. To investigate the thermal stability and decomposition behavior of the PWPU films, the TGA of polyurethanes films were conducted. As shown in Figure 6a and Table S4, the degradation process of polyurethane films includes two stages, i.e., the decomposition of hard segments formed by urethane and urea linkages and the cleavages of soft segments[39]. All the films show no significant mass loss below 250 ℃, demonstrating their good thermal stability. In contrast, the maximum mass loss temperature in first

stage (T_{1max}) shift from 296 °C (SPU) to 312 °C (PWPU-2.5) and this can be attributed to the high thermal stability and barrier properties of the introduced SiO_2-2.8.[42] Meanwhile, the hydrogen bond interactions between SiO_2-2.8 nanoparticles and polyurethane chains also contribute to the increased thermal stability (Figure 3k). With further increasing the content of SiO_2-2.8, no significant difference in the T_{1max} of PWPU samples is observed. Moreover, T_{2max} of SPU and PWPU samples is basically the same (Table S4), indicating that introducing of SiO_2 mainly affect the decomposition of the hard segment rather than soft segment of PU[45].

To gain insight into the effect of the SiO_2-2.8 content on the mechanical properties of PWPU films, tensile testing was carried out as shown in Figures 6b-d and Table S4. Compared with SPU and SPWU films, both PWPU-2.5 and PWPU-5.0 films exhibit better mechanical properties as reflected by the higher TS and EB values, confirming the reinforcement of SiO_2-2.8. This can be probably verified by the following three reasons. Firstly, the hydrogen bonding interactions between SiO_2-2.8 and polyurethane chains lead to the formation of cross-linked network in PWPU composite films[46]. Secondly, SiO_2-2.8 is able to absorb and transfer and the stress in PWPU matrix, thus preventing the formation and development of cracks[47]. Besides, the honeycomb structure within the films may also limit the crack growth[48]. However, the TS and EB values of PWPU films are slightly reduced with further increasing the content of SiO_2-2.8. The excessive SiO_2-2.8 (>7.5 wt%) would cause the formation of aggregates with voids and these voids are prone to become stress concentration points and crack initiation points under high stress conditions, ultimately resulting in the decreased mechanical property [49].

Water uptake of films cured from waterborne polymer emulsions is an important characteristic for coatings application in particular for exterior use [50]. Figure 6e presents the water uptake of SPU, SWPU and PWPU films. It is surprisingly that all the PWPU films show very low water absorption (⩽6%), almost as low as that of SPU film. The SWPU film with DMPA content of 5 wt% has the highest water uptake (WAR =101.8%). In contrast, the water absorption of PWPU-5 film is only 4.8%, approximately 20 times lower than that of SWPU film. This shows that the introduction of SiO_2 nanoparticles via Pickering emulsion approach limits the water adsorption of polyurethane significantly, contributing to the enhanced water-resistance of the cured film. This is possibly attributed to the results of the obstacles that the SiO_2-2.8 nanoparticles cause to water diffusion and the impact of the honeycomb structure on limiting the swelling of the polyurethane chains[19]. On the other hand, as the SiO_2 content increases, the water uptake of PWPU films presents a trend of increasing firstly and decreasing afterward. This observation may be the consequence of the balance between the hydrophilic feature of hydroxyl groups on SiO_2 and the limitation on the swelling of polyurethane provided by the honeycomb structures[19].

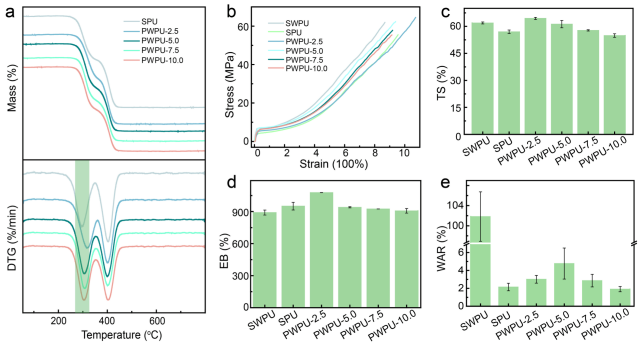

Figure 6 (a) TGA and DTG curves, **(b)** stress-strain curves, **(c)** tensile strength, **(d)** elongation at break, and **(e)** water absorption rate of SWPU, SPU, and PWPU films.

3.6 Leather coating application of PWPU composite film

Considering the stability and conversion rate of PWPU dispersions, the overall film performances of cured films, PWPU-5 was selected for leather finishing. The surface wettability of the coated leather characterized by contact angle meter is shown in Figure 7a. The water contact angle values of SWPU, and SPU coated leather are 84°±1°, and 105°±3°, respectively. It is reasonable that the hydrophobicity of SWPU is lower than SPU owing to the presence of hydrophilic chain extender DMPA in SWPU. After introduction 5 wt% SiO_2-2.8 into SPU via Pickering emulsion approach, the water contact angle value of the films (i.e., PWPU-5) increases to 113°±2°, indicating an enhancement in the hydrophobicity. This is possibly related to the increased surface roughness of PWPU-5 film provided by SiO_2-2.8 nanoparticles as corroborated by SEM. The excellent surface hydrophobicity of PWPU-5 can endow leather with good water and stain resistance.

The coatings with good abrasion resistance can ensure leather durability and esthetic appearance under daily use conditions. As shown in Figure 7b, the surfaces of SWPU and SPU coated leather are damaged obviously after abrasion test, while PWPU coated leather have slight change in brightness and no wear marks is observed. Moreover, the wear mass loss of SWPU, SPU and PWPU-5 coated leather is 54.0±1.4 mg, 39.0±1.4 mg, and 10.5±0.7 mg, respectively (Figure 7c). The lower wear mass loss of PWPU-5 coated-leather than that of SPU indicates its better abrasion resistance. It suggests that the introduction of SiO_2-2.8 into polyurethane can endow the films with outstanding abradability. The

reason is due to the fact that SiO_2-2.8 nanoparticles in PWPU-5 film is able to transfer the applied load during the wear process[51]. On the other hand, SiO_2-2.8 also can prevent fatigue crack nucleation and growth in a PU matrix due to the interfacial interaction and hydrogen bond between the nanoparticles and PU matrix[52]. PWPU-5 film with good abrasion resistance can protect leather against wear and friction.

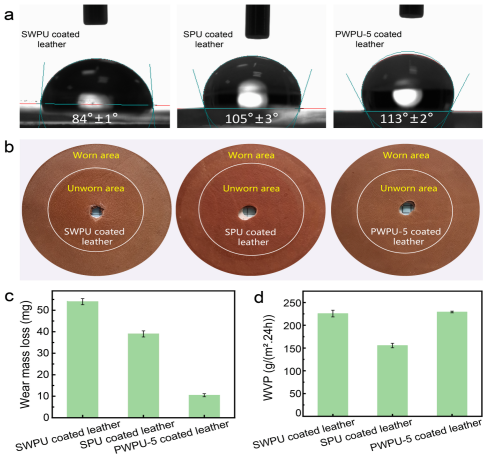

Figure 7 (a) water contact angles, **(b)** appearance (before and after abrasion test), **(c)** wear mass loss, **(d)** water vapor permeability of SWPU, SPU, and PWPU-5 coated leather.

Hygiene performance plays a very critical role in the wearing comfort of leather shoes and garments. In order to study the effect of the presence of SiO_2 nanoparticles on the hygiene performance of the coated leather, the water vapor permeability (WVP) of SWPU, SPU, and PWPU-5 coated leather was studied. As shown in Figure 7d, the WVP reduces from 225.7±7.4 g/(m^2·24h) for SWPU-coated leather to 115.5±4.9 g/(m^2·24h) for SPU coated leather. This is reasonable as the presence of hydrophilic segments (DMPA) are conductive to the transfer of water vapor within polyurethane films[53]. However, the WVP of PWPU-5 coated leather is as high as 230.1±1.9 g/(m^2·24h), which is even higher than that of SWPU-coated leather. It suggests that the presence of SiO_2-2.8 into the polyurethane matrix would not affect the water vapor permeability adversely. This may be because that the introduction of SiO_2-2.8 may impact the polyurethane network and the presence of organic-inorganic interface as well as the hydroxyl groups on SiO_2 is also in favor of the diffusion of water vapor molecules[7]. As a result, the suitable WVP of PWPU-5 give leather garments preferable wearing comfort.

4. Conclusions

The Pickering waterborne polyurethane emulsion (PWPU) was successfully fabricated by using SiO_2 nanoparticles as Pickering stabilizer. The good Pickering emulsion effects can be achieved by the optimized hydrophobic modification of SiO_2, as verified by the excellent emulsion stability of PWPU. The PWPU films present high transparency and morphology of honeycomb structures, revealing that the Pickering stabilizer would not hinder the film formation process of PWPU if cured at room temperature. The film performance of PWPU particularly the mechanical property and thermal stability are comparable or even higher than those of the solvent-based polyurethane and self-emulsifying waterborne polyurethane (SWPU) films. It is noted that the water uptake of the PWPU film is approximately 20 times lower than that of SWPU, demonstrating that the introduction of SiO_2 nanoparticles via Pickering emulsion approach contributes to the enhancement of water-resistance of WPU films significantly. More importantly, the leather coated with PWPU exhibits better hydrophobicity, abrasion resistance and water vapor permeability than either SPU or SWPU coated-leather. This work demonstrates that Pickering emulsion approach can be used as a potential strategy to fabricate waterborne polyurethane emulsions for film application such as leather finishing.

Acknowledgment

The financial support of National Natural Science Foundation of China (22108182, 22278277), the Fundamental Research Funds for the Central Universities (2023SCU12105) are gratefully acknowledged.

References

[1] X. Wu, J. Wu, C. Mu, C. Wang, W. Lin, Advances in antimicrobial polymer coatings in the leather industry: A comprehensive review, Ind. Eng. Chem. Res. 60, 15004-15018,2021
[2] C.H. Wang, Z.L. Yi, Y.F. Sheng, L. Tian, L. Qin, T. Ngai, W. Lin, Development of a novel biodegradable and anti-bacterial polyurethane coating for biomedical magnesium rods, Mater. Sci. Eng. C-Biomimetic Supramol. Syst. 99,344-356, 2019
[3] J. Pan, Q. Xie, H. Chiang, Q. Peng, P.-Y. Qian, C. Ma, G. Zhang, "From the nature for the nature": An eco-friendly antifouling coating consisting of poly(lactic acid)-based

polyurethane and natural antifoulant, ACS Sustain. Chem. Eng. 8, 1671-1678, 2020.
[4] H. Luo, H. Wei, L. Wang, Q. Gao, Y. Chen, J. Xiang, H. Fan, Anti-smudge and self-cleaning characteristics of waterborne polyurethane coating and its construction, J. Colloid Interface Sci. 628,1070-1081, 2022
[5] J. Sang, L. Yu, S. Xie, F. Zhang, X. Zhang, W. Lin, Simultaneous determination of N-methyl-2-pyrrolidone (NMP) and N-Ethyl-2-pyrrolidone (NEP) in leather by gas chromatography-mass spectrometry, J. Soc. Leather Technol. Chem. 99, 134-138, 2015
[6] J. Shi, R. Puig, J. Sang, W. Lin, A comprehensive evaluation of physical and environmental performances for wet-white leather manufacture, J. Clean Prod. 139 ,1512-1519, 2016
[7] K. Yan, C. Liu, J. Ma, Dendritic fibrous nanosilica loaded chitosan for improving water vapor permeability and antibacterial properties of waterborne polyurethane acrylate membranes, J. Clean Prod. 291 ,2021.
[8] C. Wang, J. Wu, L. Li, C. Mu, W. Lin, A facile preparation of a novel non-leaching antimicrobial waterborne polyurethane leather coating functionalized by quaternary phosphonium salt, J. Leather Sci. Eng. 2, 2020.
[9] J. Wu, C. Wang, W. Lin, T. Ngai, A facile and effective approach for the synthesis of fluorinated waterborne polyurethanes with good hydrophobicity and antifouling properties, Prog. Org. Coat. 159, 106405, 2021.
[10] K.-L. Noble, Waterborne polyurethanes, Prog. Org. Coat. 32, 131-136,1997.
[11] J. Faucheu, C. Gauthier, L. Chazeau, J.-Y. Cavaille, V. Mellon, E. Bourgeat-Lami, Miniemulsion polymerization for synthesis of structured clay/polymer nanocomposites: Short review and recent advances, Polymer, 51,6-17, 2010.
[12] P. Li, A. Zhang, S. Zhou, One-component waterborne *in vivo* cross-linkable polysiloxane coatings for artificial skin, J. Biomed. Mater. Res. Part B, 108, 1725-1737, 2020.
[13] P. Li, S. Wang, S. Zhou, Pickering emulsion approach for fabrication of waterborne cross-linkable polydimethylsiloxane coatings with high mechanical performance, J. Colloid Interface Sci. 585 ,2021, 627-639, 2021.
[14] H. Jiang, Y.F. Sheng, T. Ngai, Pickering emulsions: Versatility of colloidal particles and recent applications, Curr. Opin. Colloid Interface Sci. 49, 1-15, 2020.
[15] C. Wang, X. Guan, J. Sang, J. Zhou, C. Wang, T. Ngai, W. Lin, General liquid vegetable oil structuring via high internal phase Pickering emulsion stabilized by soy protein isolate nanoparticles, J. Food Eng. 356, 2023.
[16] H. Jiang, L. Hong, Y. Li, T. Ngai, All-silica submicrometer colloidosomes for cargo protection and tunable release, Angew. Chem.-Int. Edit. 57,11662-11666, 2018.
[17] Y. Bao, Y.X. Zhang, J.Z. Ma, Reactive amphiphilic hollow SiO_2 Janus nanoparticles for durable superhydrophobic coating, Nanoscale, 12, 16443-16450, 2020.
[18] Z. Chen, Y. Huang, Preparation and performance of fumed silica-stabilized epoxy resin pickering emulsion for basalt fiber-sizing agents, Adv. Compos. Hybrd. Mater , 1205-1214, 2021.
[19] K. González-Matheus, G.P. Leal, J.M. Asua, Film formation from Pickering stabilized waterborne polymer dispersions, Polymer, 69,73-82, 2015.
[20] Y. Zhang, J. Wu, B. Wang, X. Sui, Y. Zhong, L. Zhang, Z. Mao, H. Xu, Cellulose nanofibril-reinforced biodegradable polymer composites obtained via a Pickering emulsion approach, Cellulose , 24,3313-3322, 2017.
[21] J. Pavličević, M. Špírková, M. Jovičić, J. Budinski-Simendić, B. Pilić, S. Baloš, O. Bera, Structure—Functional property relationship of aliphatic polyurethane-silica hybrid films, Prog. Org. Coat. 126, 62-74, 2019.
[22] QB/T 2223-1996, Testing method for acrylic resin emulsions used in leather production 1996.
[23] GB/T 11175-2021, Testing method for synthetic resin emulsions, 2021.
[24] ASTM D882-97, Standard test methods for tensile properties of thin plastic sheeting ,1997.
[25] K. Zhang, W. Wu, H. Meng, K. Guo, J.F. Chen, Pickering emulsion polymerization: Preparation of polystyrene/nano-SiO_2 composite microspheres with core-shell structure, Powder Technol. 190, 393-400, 2009.
[26] X. Zheng, Y. Zhang, H. Wang, Q. Du, Interconnected macroporous polymers synthesized from silica particle stabilized high internal phase emulsions, Macromolecules, 47, 6847-6855, 2014.
[27] J. Wu, C. Wang, W. Lin, T. Ngai, A facile and effective approach for the synthesis of fluorinated waterborne polyurethanes with good hydrophobicity and antifouling properties, Prog. Org. Coat. 159, 2021.
[28] J. Wu, X. Guan, C. Wang, T. Ngai, W. Lin, pH-Responsive Pickering high internal phase emulsions stabilized by waterborne polyurethane, J. Colloid Interface Sci. 610 (2022) 994-1004.
[29] X. Shang, Y. Jin, W. Du, L. Bai, R. Zhou, W. Zeng, K. Lin, Flame-retardant and self-healing waterborne polyurethane based on organic selenium, ACS Appl. Mater. Interfaces, 15, 16118-16131, 2023.
[30] C. Ma, X. Bi, T. Ngai, G. Zhang, Polyurethane-based nanoparticles as stabilizers for

oil-in-water or water-in-oil Pickering emulsions, J. Mater. Chem. A 1, 5353-5360, 2023
[31] Y. Sheng, K. Lin, B.P. Binks, T. Ngai, Ultra-stable aqueous foams induced by interfacial co-assembly of highly hydrophobic particles and hydrophilic polymer, Colloid Interface Sci. 579, 628-636, 2020
[32] M. Okada, H. Maeda, S. Fujii, Y. Nakamura, T. Furuzono, Formation of Pickering emulsions stabilized via interaction between nanoparticles dispersed in aqueous phase and polymer end groups dissolved in oil phase, Langmuir, 28, 9405-9412, 2012
[33] X. Cai, C. Li, Q. Tang, B. Zhen, X. Xie, W. Zhu, C. Zhou, L. Wang, Assembling kaolinite nanotube at water/oil interface for enhancing Pickering emulsion stability, Appl. Clay Sci. 172,115-122,2019
[34] C. Linke, S. Drusch, Pickering emulsions in foods - opportunities and limitations, Crit. Rev. Food Sci. Nutr. 58, 1971-1985,2018.
[35] L. Chen, F. Ao, X. Ge, W. Shen, Food-grade Pickering emulsions: Preparation, stabilization and applications, Molecules 25, 2020.
[36] A. Khan, K. Huang, M.G. Sarwar, M. Rabnawaz, High modulus, fluorine-free self-healing anti-smudge coatings, Prog. Org. Coat. 145 , 2020,105703, 2020
[37] J. Ma, C. Liu, Y. Zhang, Y. Dong, C. Liu, Z. Ma, The influence of hydrogen bond and electrostatic interaction on the mechanical properties of the WPU/modified SiO2 nanocomposites, Colloids Surf. Physicochem. Eng. Aspects 648, 129364, 2022
[38] J. Ma, K. Cai, C. Yang, M. Li, X. Pan, Y. Huang, J. Yao, J. Zheng, J. Shao, Synthesis and properties of photocurable polyurethane acrylate for textile artificial leather, Prog. Org. Coat. 171,107017, 2022
[39] J.H. Wu, C.H. Wang, C.D. Mu, W. Lin, A waterborne polyurethane coating functionalized by isobornyl with enhanced antibacterial adhesion and hydrophobic property, Eur. Polym. J. 108, 498-506, 2018.
[40] J.I. Amalvy, M.J. Percy, S.P. Armes, H. Wiese, Synthesis and characterization of novel film-forming vinyl polymer/silica colloidal nanocomposites, Langmuir, 17, 4770-4778, 2001
[41] A. Schmid, P. Scherl, S.P. Armes, C.A.P. Leite, F. Galembeck, Synthesis and characterization of film-forming colloidal nanocomposite particles prepared via surfactant-free aqueous emulsion copolymerization, Macromolecules, 42, 3721-3728, 2009
[42] N. Negrete-Herrera, J.-L. Putaux, L. David, F. De Haas, E. Bourgeat-Lami, Polymer/Laponite composite latexes: Particle morphology, film microstructure, and properties, Macromol. Rapid Commun. 28, 1567-1573, 2007
[43] E. Gonzalez, A. Bonnefond, M. Barrado, A.M. Casado Barrasa, J.M. Asua, J.R. Leiza, Photoactive self-cleaning polymer coatings by TiO_2 nanoparticle Pickering miniemulsion polymerization, Chem. Eng. J. 281, 209-217, 2015
[44] Y. Zhang, H. Yang, N. Naren, S.J. Rowan, Surfactant-free latex nanocomposites stabilized and reinforced by hydrophobically functionalized cellulose nanocrystals, ACS Appl. Polym. Mater. 2, 2291-2302, 2020
[45] C. Salgado, M.P. Arrieta, L. Peponi, D. López, M. Fernández-García, Photo-crosslinkable polyurethanes reinforced with coumarin modified silica nanoparticles for photo-responsive coatings, Prog. Org. Coat. 123, 63-74, 2018
[46] H. Fu, C. Yan, W. Zhou, H. Huang, Preparation and characterization of a novel organic montmorillonite/fluorinated waterborne polyurethane nanocomposites: Effect of OMMT and HFBMA, Compos. Sci. Technol. 85, 65-72, 2013
[47] X. Wu, Y. Liao, G. Meng, L. Tang, Z. Zhou, Q. Li, W. Huang, SiO_2/carbon fiber-reinforced polypropylene-thermoplastic polyurethane composites: electrical conductivity and mechanical and thermal properties, Iran. Polym. J. 28, 527-537, 2019
[48] K. Gonzalez-Matheus, G. Patricia Leal, J.M. Asua, Film formation from Pickering stabilized waterborne polymer dispersions, Polymer, 69,73-82,2015
[49] R.C.R. Nunes, J.L.C. Fonseca, M.R. Pereira, Polymer-filler interactions and mechanical properties of a polyurethane elastomer, Polym. Test. 19, 93-103,2000
[50] Q. Zhang, Y. Zhou, J. Ma, H. Wang, W. Li, Synthesis and coating properties of sulfonated calixarene-based waterborne polyurethane hydrotalcite nanocomposite, Polym. Adv. Technol. 34, 1653-1661,2023.
[51] W. Fan, W. Du, Z. Li, N. Dan, J. Huang, Abrasion resistance of waterborne polyurethane films incorporated with PU/silica hybrids, Prog. Org. Coat. 86, 125-133,2015
[52] M. Malaki, Y. Hashemzadeh, A.F. Tehrani, Abrasion resistance of acrylic polyurethane coatings reinforced by nano-silica, Prog. Org. Coat. 125, 507-515, 2018
[53] X. Hou, H. Zhao, W. Zhang, H. Ma, R. Li, B. Han, Y. Zhang, J.-J. Wang, Moisture-regulating microcapsule and its enhanced water vapor permeability of leather polyurethane coating, Prog. Orga. Coat. 166, 2022.